Cheju Journal of Medicine
Vol. 1, No. 1. 25-33, December 2003

Identification of novel mutations in three Korean families with X-linked chronic granulomatous disease

Kyung-Sue Shin

Department of Pediatrics, College of Medicine, Cheju National University, Jeju 690-756, Korea

Abstract: Chronic granulomatous disease (CGD) is a rare hereditary disorder due to defective activity of phagocytic NADPH oxidase. Defects in gp91-*phox* subunit of cytochrome b_{558} give rise to X-linked CGD, which caused by mutations in the CYBB gene on Xp21.1. Although approximately 300 different mutations of the CYBB gene have been identified, the distribution of mutations within CYBB gene shows a great heterogeneity. The mutations in the CYBB gene of four Korean patients with X-linked CGD from three unrelated families were identified in this study. Mutations were screened by single-strand conformation polymorphism (SSCP) and then confirmed by sequence analysis. Three different mutations were identified: one missense mutations (G1473 → T), one nonsense mutations (G1235 → T), and a splice site mutation at intron 11 resulting in the whole absence of exon 11 (5'gt → tt). These mutations are novel mutations. In this study, mutations of the X-linked CGD are very heterogeneous and do not have the peculiarity of the ethnic group.

Key words: Chronic granulomatous disease, CYBB gene, gp91-phox, novel mutation

INTRODUCTION

Chronic granulomatous disease (CGD) is a rare X-linked or autosomal recessive disease characterized by recurrent life-threatening infections and granuloma formation. The underlying defect of CGD is an inability of phagocytes to produce superoxide (O_2^-) as a result of the defect in one of the subunit of NADPH oxidase; p47-*phox*, p67-*phox*, p22-*phox*, gp91-*phox*, and p40-*phox* (1). Superoxide is a kind of microbicidal oxidants that are critical to the destruction of invading microorganisms by phagocytes (2).

X-linked CGD (X-CGD) is the most common type of CGD and caused by mutations in the gp91-*phox* of the NADPH oxidase. The gene for gp91-*phox*, termed as CYBB (the β subunit of cytochrome b_{558}), was identified by positional cloning (3), following chromosomal localization to Xp21.1 (4). The CYBB gene encompasses approximately 30 kb, and contains 13 exons. The gp91-*phox* contains 570 amino acids, with four or five transmembrane helices and five potential N-liked glycosylation sites in the N-terminal domain. C-terminal domain contains the putative NADPH- and FAD-binding sites and loop over the NADPH-binding domain (5-7). The muta-

*Corresponding author: kyungsue@cheju.ac.kr

tions identified in the present studies appear almost uniformly throughout gp91-*phox* molecule, with a slight predominance in the N-terminal domain (7-10). In this study of four Korean patients from three families, three different mutations in the gene of gp91-*phox* were newly identified.

MATERIALS AND METHODS

Patients — **4** patients and nine family members of patients were included in this study. The diagnosis of X-linked CGD was based on the history of recurrent infections and previously affected family member and was confirmed by the NBT reduction test for each patient and their family members. All mothers, one of them came from the same family, two maternal grandmothers, two maternal aunts from three unrelated X-CGD families showed a mosaic pattern of the NBT reduction test, which agrees with X-linked pattern of inheritance (Table 1).

Table 1. The results of NBT reduction test in three unrelated families

		Reduced granulocytes (% of total granulocytes)
Family I	Patient 1	0
	Mother	80
	Sister	83
	Maternal aunt	60
	Maternal grandmother	54
Family II	Patient 2	0
	Patient 3	0
	Mother	15
	Maternal grandmother	65
Family III	Patient 4	0
	Mother	48
	Maternal aunt	40
	Brother	100

Isolation of genomic DNA and total RNA — Genomic DNA and total RNA were extracted from the Epstein-Barr virus (EBV)-transformed patient or normal B-cell lines. Peripheral blood mononuclear cells isolated by Ficoll-Hypaque (Lymphoprep™; Nycomed Pharma AS, Oslo, Norway) sedimentation were transformed with EBV-containing supernatant from B95-8 marmoset cell line as described by Neitzel (11). For isolation of genomic DNA, the genomic DNA purification kit (Wizard®; Promega, Madison, WI) was used according to the protocol provided. Using TRIzol® reagent (GIBCO-BRL, Gaithersburg, MD), total RNA was isolated as recommended by the manufacturer.

Reverse transcription-PCR (RT-PCR) — Reverse transcription was performed in a 20 μL reaction mixture containing 50 mM Tris (pH 8.3), 40 mM KCl, 8 mM $MgCl_2$, 10 mM dithiothreitol, 500 μM of each dNTPs, 20 U RNase inhibitor (Promega, Madison, WI), 40 μg/mL oligo(dT)15 primer (Promega, Madison, WI), 1 μg total RNA, and 100 U of AMV reverse transcriptase (Promega, Madison, WI). The mixture was incubated at 42℃ for 60 min, then inactivated by heating to 95℃ for 10 min. Using three pairs of synthetic oligonucleotide primers as described by Dinauer et al. (12), cDNA were PCR-amplified in a 50 μL reaction mixture containing 10 pM of each primer, 200 μM dNTPs, 100 mM Tris-HCl, pH 8.3, 50 mM KCl, 1.5 mM $MgCl_2$, and 2.5 U Taq polymerase (Promega, Madison, WI). The amplification conditions were as follow: 94℃ for 60 seconds, 56℃ for 90 seconds, and 72℃ for 60 seconds, for a total 30 cycles with a extension at 72℃ for 10 minutes.

PCR of genomic DNA — The 5' flanking region and each exon/intron boundary of the CYBB gene was amplified using a pair of synthetic oligonucleotide primers provided by Dr. A. R. Cross. Exon 9 was amplified in two overlapping fragments. Genomic DNA were PCR-amplified in a 50 μL reaction mixture containing 10

pM of each primer, 200 μM dNTPs, 100 mM Tris-HCl, pH 8.3, 50 mM KCl, 1.5 mM $MgCl_2$, and 2.5 U Taq polymerase (Promega, Madison, WI). The amplification conditions were as follow: 94℃ for 30 seconds, 58℃ for 30 seconds, and 72℃ for 30 seconds, for a total 30 cycles with a extension at 72℃ for 7 minutes. The annealing temperature of exon 6 was 55℃.

SSCP analysis – SSCP analysis was performed on the 5' flanking region and all 13 exon/intron boundaries of the CYBB gene. Each PCR product was mixed with two times of SSCP loading buffer (95% [vol/vol] formamide, 0.5% [wt/vol] bromphenol blue, 0.5% [wt/vol] xylene cyanol, 20 mM EDTA, 0.1% [wt/vol] sodium dodecyl sulfate), denatured at 95℃ for 10 minutes, and stored on ice for 10 minutes. A mixture was electrophoresed at 300 - 350 V at room temperature for 15 hours or 500 V at the cold room overnight. The 8% to 12% non-naturing polyacrylamide gels were used and the running buffer of electrophoresis was 0.5 X TBE buffer. The gel was stained by the silver staining procedure with slight modifications as described by Mitchell et al. 13). Briefly, the gel was soaked in 10% (vol/vol) ethanol for 10 minutes and then placed in 2% (vol/vol) concen-ated nitric acid for 5 minutes. After washing the gel three times with deionized water, the gel was placed in 2% (vol/vol) silver nitrate solution for 20 minutes. A washed gel with deionized water was developed with precooled mixture of the 0.28 M sodium carbonate and formaldehyde until the gel image had formed. The development of the image was stopped by 10% (vol/vol) acetic acid for 15 minutes. The gel was dried on filter paper under vacuum with heating. The migration patterns were compared with patients and normal control; exon/ntron boundaries with aberrant migration pattern were sequenced.

DNA sequencing and Sequence alignment – The PCR products were purified with a PCR product purification kit (QIAquick™; QIAGEN, Hilden, Germany) and sequence analyses were performed using an ABI PRISM 377 automatic sequencer. Each fragment of the PCR products was sequenced in both directions. All sequences were aligned with both the standard sequence (provided by Dr. A. R. Cross) and the sequence of a normal control using the BLAST 2 sequences (www.ncbi.nlm.nih.gov/BLAST).

RESULTS

The mRNA of gp91-phox in patients and family members to investigate whether their mutations were large gene deletions or splice site errors were analyzed. The mRNAs of gp91-phox were reverse transcribed into three overlapping cDNA fragments as described above. The PCR fragments of cDNA in patients and family members showed no abnormal fragments compared with the normal control except patient 1. In patient 1, the PCR fragment III of cDNA containing from exon 9 to exon 13 was apparently smaller (about 550 bp) than the normal fragment (694 bp). Two coinciding fragments were observed for fragment III in his mother, in agreement with the carrier status. To investigate whether the absence of his exonal sequence was due to gene deletion or splice site error, his smaller cDNA fragment was sequenced. The result showed exon 10 directly joined to exon 12 with whole absence of exon 11 (140 bp). When the exon/intron boundary of the missing exon was sequenced, a single base substitution of g to t was observed at +1 position of 5' splice site in intron 11. This point mutation of intron 11 caused a splice site error (Fig. 1).

The 5' flanking region and all 13 exon/intron boundaries of the CYBB gene were analyzed by SSCP

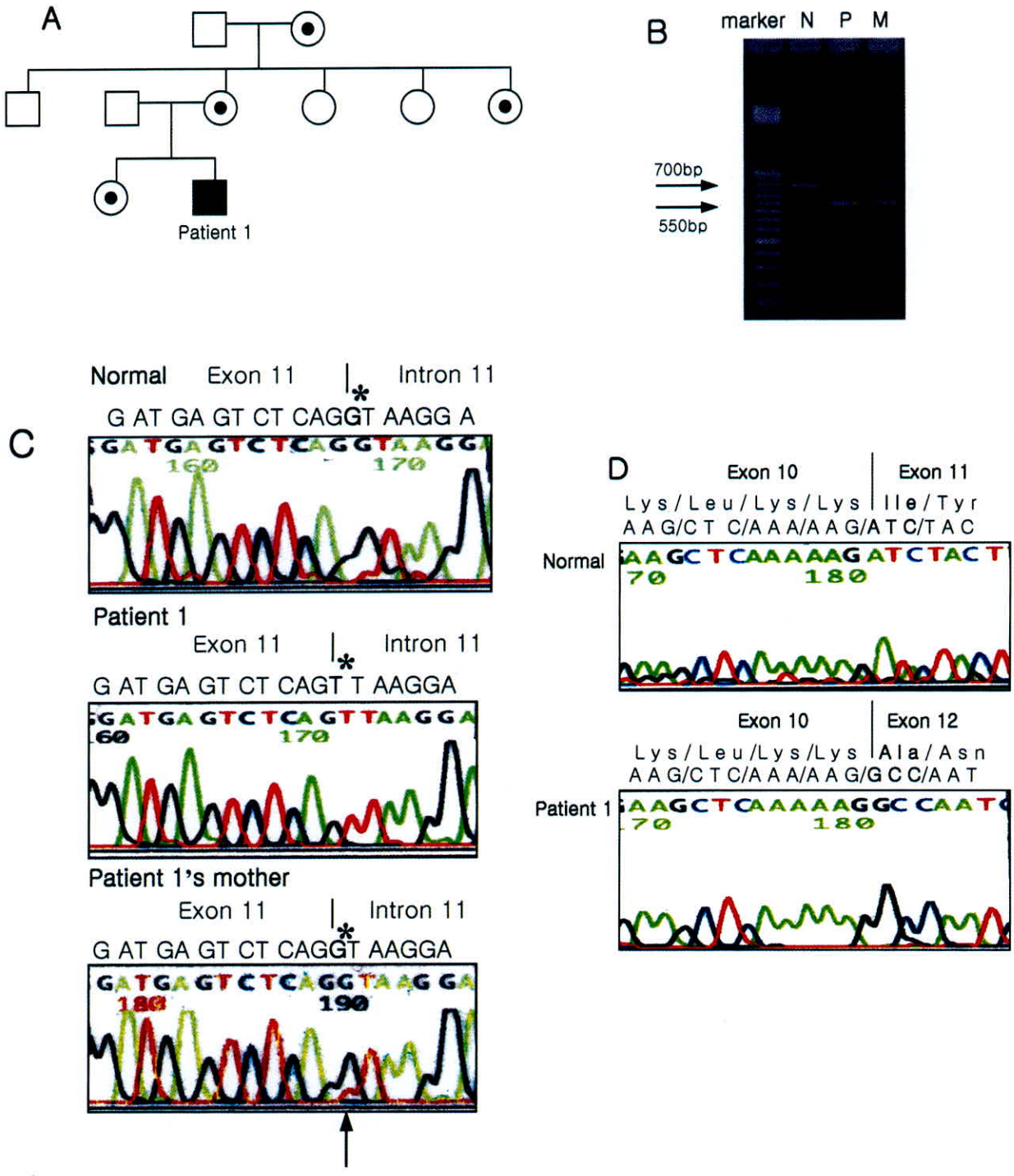

Fig. 1. A: The pedigree of patient 1. B: Size analysis of the amplified third fragment of gp91-*phox* cDNA in patient 1. The molecular size marker is from 150 to 800 bp with 50-bp difference. Each lane is as follows: N, normal control; P, patient 1; M, mother of patient 1. The cDNA fragment of patient 1 showed a smaller (about 550 bp) than that of normal control. His mother gave both the smaller and normal fragments (694 bp). C: Sequence analysis of exon 11/intron 11 boundary. Sequence analysis showed a g (+1) → t transition in patient 1. D: Sequence analysis of the third fragment of gp91-*phox* cDNA in patient 1. The analysis showed exon 10 joined directly to exon 12 with whole absent exon 11.

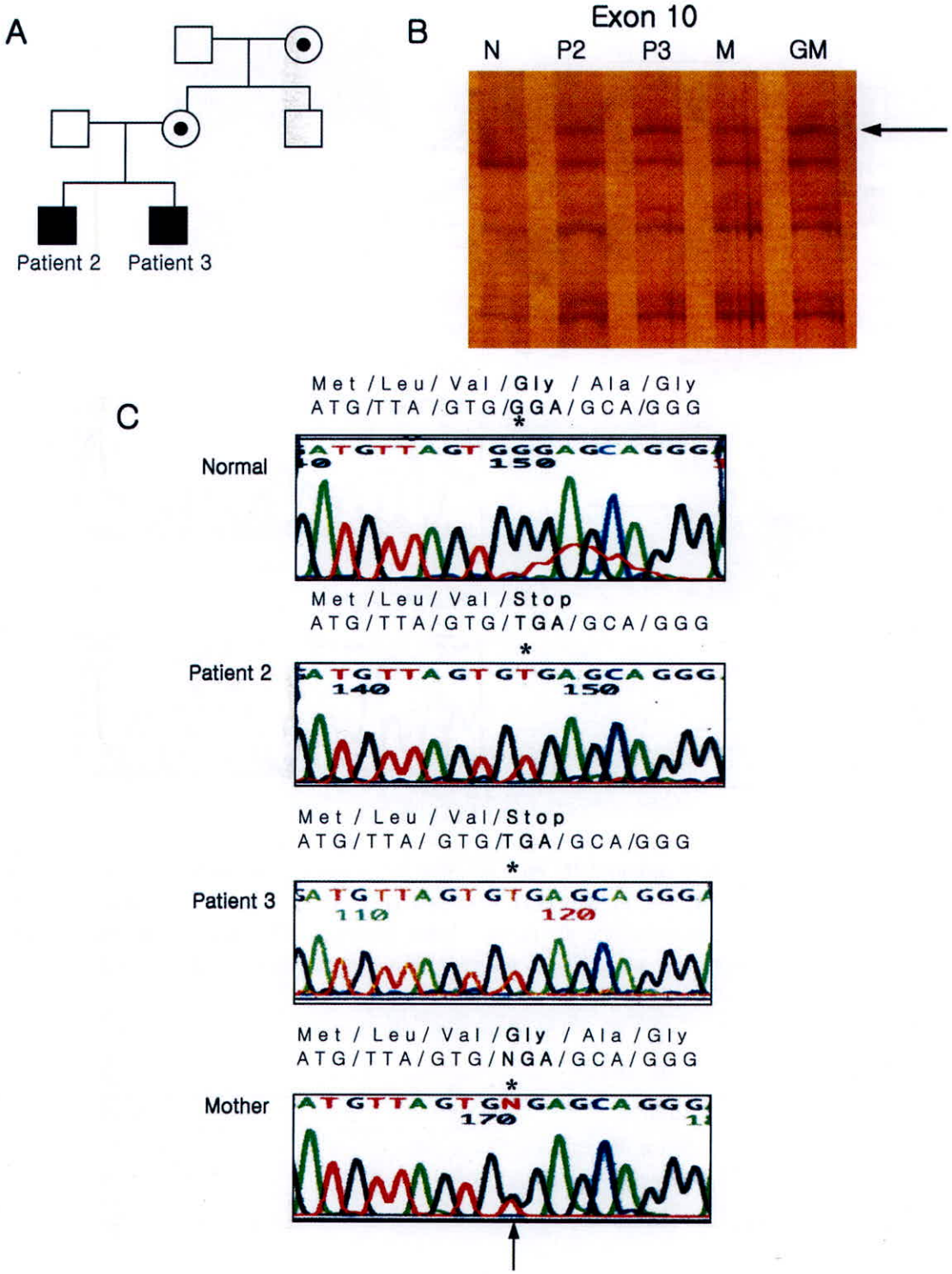

Fig. 2. A: The pedigree of patient 2 and 3. B: SSCP of exon 10. Each lane is as follows: N, normal control; P2, patient 2; P3, patient 3; M, mother; GM, maternal grandmother. An arrow indicates abnormally additional aberrant bands. C: Sequence analysis of exon 10. Asterisks indicate a G1235 → T transition in patient 2 and patient 3 resulted in a nonsense mutation Gly 408 (GGA) → stop codon (TGA). Sequence analysis of his mother showed the double signal at the position of nucleotide 1235 (arrow), which showed the heterozygosity of his mother.

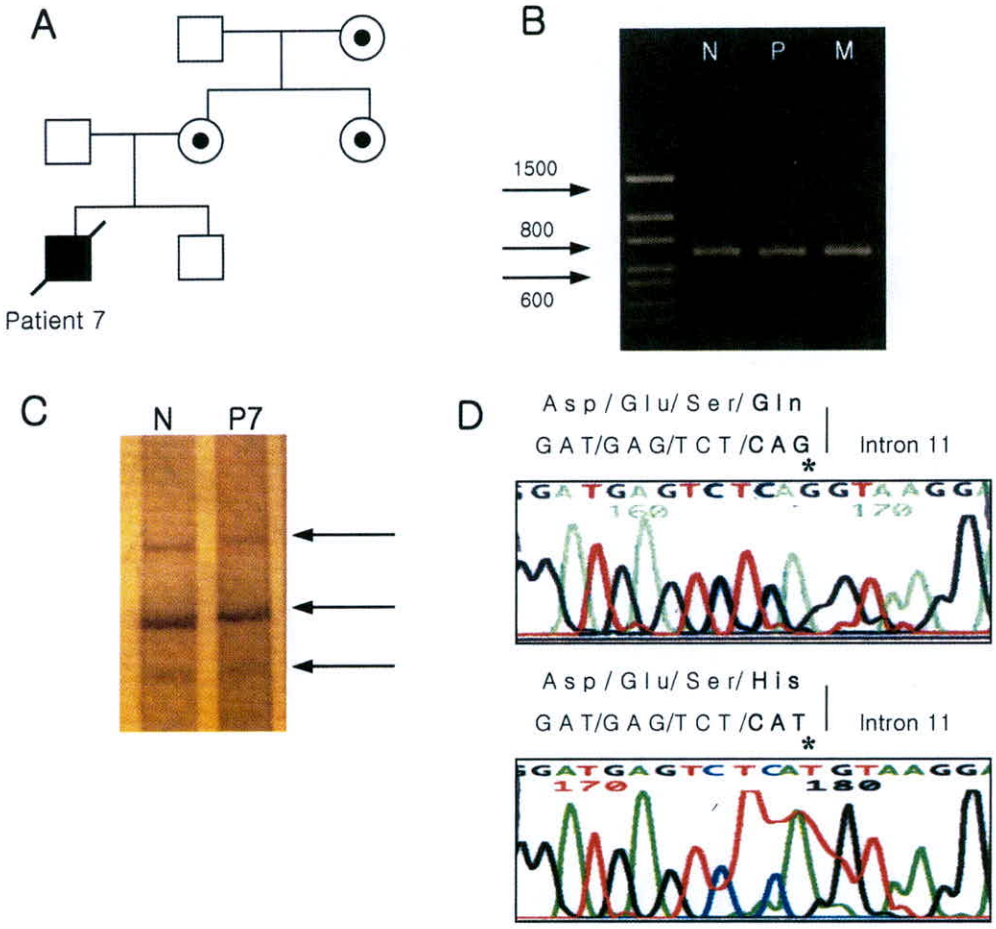

Fig. 3. A: The pedigree of patient 4. B: Size analysis of the amplified third fragment of gp91-*phox* cDNA in patient 4. The molecular size marker is from 300 to 1500 bp. Each lane is as follows: N, normal control; P, patient 4; M, mother of patient 4. The cDNA fragment III of patient 4 showed no abnormal fragments compared with the normal control. C: SSCP of exon 11. Arrows indicate abnormally slower migrations. D: Sequence analysis of exon 11. A G1473 → T transition in patient 4 is marked with asterisk. This point mutation resulted in a missense mutation Gln487 → His.

Table 2. Three families and identified mutations

Family No.	Mutation Site	Mutation	Nucleotide Change	Amino Acid change
1	Intron 11	Splice site error	5gt→ tt	Deletion exon 11
2	Exon 10	Nonsense	G1235 → T	Gly (GGA)408 → Stop (TGA)
3	Exon 11	Missense	G1473 → T	Gln (CAG)487 → His (CAT)

for screening mutations. In patient 2 and 3, a clear aberrant band in the SSCP analysis of exon 10 was detected. In patient 4, an abnormally slower migrating band in exon 11 was observed in SSCP analysis.

The exon/intron boundaries that showed abnormal migrating bands in SSCP analysis were sequenced. One missense mutation (G1473 → T) and one nonsense mutations (G1235 → T) in two unrelated families were identified.

Patient 2 and 3 are brothers; a single base substitution of G1235 to T was found in exon 10, which

resulted in a nonsense mutation Gly 408 (GGA) → stop codon (TGA). Sequence analysis of his mother showed the double signal at the position of nucleotide 1235, which showed her carrier status (Fig. 2).

In patient 4, a G1473 → T substitution in the last base of exon 11 was found. This change results in a missense mutation Gln487 → His (Fig. 3). Table 2 summarizes identified three mutations from unrelated families.

DISCUSSION

In this study, three different mutations of the CYBB gene in three families with X-CGD were identified. Screening by SSCP analysis identified abnormalities; sequence analysis of genomic DNA confirmed mutations in three families. SSCP analysis used in this study had higher sensitivity to detect mutations in spite of using the silver staining method instead of radioisotpe for detecting electrophoretic band profile.

Splice site selection in pre-mRNA occurs by recognition of consensus sequences located on the intron side of each splice site. Each intron begins with gt dinucleotide and ends with ag dinucleotide (14, 15). In the most splice site mutations, mutations in the gt dinucleotide at the 5' splice site predominated, which could lead to either alternative splicing using of cryptic splice sites or exonal skipping 15). Robberson et al. 16) proposed exon boundaries were firstly recognized during splicesome assembly (exon definition) and failing of exon definition would result in exon skipping. Analysis of genomic DNA in patient 1 showed that exon 11 were not deleted in the gene and a single nucleotide g was substituted to t at +1 position in 5' splice site of intron 11. The gt dinucleotide in intron 11 changed to tt dinucleotide, which apparently causes aberrant mRNA with skipping exon 11. However, in patient 4, a G1473 → T substitution in the last base of exon 11 was found. The PCR fragments of cDNA in patient 4 showed no abnormal fragments compared with the normal control (Fig. 3). A G1473 → T transition resulted in not a splice site mutation but a missense mutation.

Exon 11 encodes NADPH binding domain and a part of loop over the NADPH-binding domain in gp91-*phox* (7). Interaction of p47-*phox* and/or p67-*phox* with cytochrome b_{558} may result in movement of the loop over the NADPH-binding domain and in access of NADPH to binding site in gp91-*phox* during phagocyte activation (17). Thus, absence of exon 11 in patient 1 may result in producing an unstable truncated protein that will not be interacted with p47-*phox* and/or p67-*phox* and be absent in the expression of gp91-*phox*. Most of splice site mutations in X-CGD lead to $X91^0$ phenotype as with patient 1 (8).

Patient 4 suffered multiple infections during first year of life: cervical lymphadenitis, perianal abscess, fungal pneumonia by *Candida albicans*, spleen abscess by *Staphylococcus aureus*, septicemia by coagulase-negative *Staphylococcus*, and died at age of 40 months as a result of sepsis. In patient 4, a G1473 → T substitution in the last base of exon 11 was found. This change results in a missense mutation Gln487 → His. The loop over the NADPH-binding domain (Asp408-Thr503) covers the cleft in which NADPH binds to gp91-*phox*. The NADPH binding domain is accessible for NADPH only when the loop moves aside after interaction with p67-*phox* (7). Only a few mutations in this loop have been found (18). Substitution of Gln487 to His may produce the conformational change of the loop, which may prevent a series of interaction with p67-*phox*. Further investigations should be performed to clarify altered structure and function of gp91-*phox* by this mutation.

The best-known mechanism of single nucleotide substitutions is methylation-induced deamination of cytosine

in CpG sequence, which leads to thymidine formation. In this study, two G → T transversions identified in patient 2, 4 which is not restricted to CpG sequences.

In patient 2 and 3, a single nucleotide transition of G1235 to T was found in exon 10, which resulted in a nonsense mutation Gly 408 → stop codon. This site was also reported that four patient from three unrelated families had the same missense mutation G1235 → A (Gly 408 → Glu). Nonsense mutations in patient 2 and 3 may produce a truncated protein that will be unstable and easily degraded as other patients.

In summary, three different mutations of the CYBB gene in Korean patients give rise to X-CGD. All mutations are novel mutations. The three mutations are located in three different position of CYBB gene and are different to each family. This heterogeneity is also found in other ethnic groups, which suggest the absence of ethnic group-specific mutation. This results may confirm that mutations of the X-linked CGD are very heterogeneous and do not have the peculiarity of the ethnic group.

ACKNOWEDGEMENTS

I am grateful to Dr. Andrew R. Cross, Department of Molecular and Experimental Medicine, The Scripps Research Institute, La Jolla, CA, for providing the se= quences of intron-exon boundaries and the corresponding primer sequences of the CYBB gene.

REFERENCES

1. Smith RM, Curnutte JT. Molecular basis of chronic granulomatous disease. *Blood* 1991;77:673-686.
2. Segal BH, Leto TL, Gallin JI, et al. Genetic, biochemical, and clinical features of chronic granulomatous disease. *Medicine (Baltimore)* 2000;79:170-200.
3. Royer-Pokora B, Kunkel LM, Monaco AP, et al. Cloning the gene for an inherited disorder- chronic granulomatous disease- on the basis of its chromosomal location. *Nature* 1986;322:32-38.
4. Baehner RL, Kunkel LM, Monaco AP, et al. DNA linkage analysis of X chromosome-linked chronic granulomatous disease. *Proc Natl Acad Sci USA* 1986;83:3398-3401.
5. Dinauer MC, Orkin SH, Brown R, et al. The glycoprotein encoded by the X-linked chronic granulomatous disease locus is a component of the neutrophil cytochrome b complex. *Nature* 1987; 327:717-719.
6. Teahan C, Rowe P, Parker P, et al. The X-linked chronic granulomatous disease gene codes for the beta chain of cytochrome b_{245}. *Nature* 1987;327: 720-721.
7. Roos D, Curnutte JT, Hossle JP, et al. X-CGD base: a database of X-CGD-causing mutations. *Immunol Today* 1996;17:517-521.
8. Rae J, Newburger PE, Dinauer MC, et al. X-linked chronic granulomatous disease: mutations in the CYBB gene encoding the gp91-*phox* component of respiratory-burst oxidase. *Am J Hum Genet* 1998;62:1320-1331.
9. Heyworth PG, Curnutte JT, Rae J, et al. Hematologically important mutations: X-linked chronic granulomatous disease-an update. *Blood Cells Mol Dis* 1997;23:443-450.
10. Roos D, de Boer M, Kuribayashi F, et al. Mutations in the X-linked and autosomal recessive forms of chronic granulomatous disease. *Blood* 1996;87: 1663-1681.
11. Neitzel H. A routine method for the establishment of permanent growing lymphoblatoid cell lines. *Hum Genet* 1986;73:320-326.

12. Dinauer MC, Curnutte JT, Rosen H, et al. A missense mutation in the neutrophil cytochrome b heavy chain in cytochrome-positive X-linked chronic granulomatous disease. *J Clin Invest* 1989;84:2012-2016.
13. Mitchell LG, Bodenteich A, Merril CR. Use of silver staining to detect nucleic acids. *Methods Mol Biol* 1994;31:197-203.
14. Sharp PA. Splicing of messenger RNA precursors. *Science* 1987;235:766-771.
15. Lewin B. Alternatives for splicing: recognizing the ends of intron. *Cell* 1980;22:324-326.
16. Robberson BL, Cote GJ, Berget SM. Exon definition may facilitate splice site selection in RNAs with multiple exons. *Mol Cell Biol* 1990;10:84-94.
17. Seger RA, Tiefenauer L, Matsunaga T, et al. Chronic granulomatous disease due to granulocytes with abnormal NADPH oxidase activity and deficient cytochrome-b. *Blood* 1983;61:423-428.
18. Leusen JH, de Boer M, Bolscher BG, et al. A point mutation in gp91-*phox* of cytochromeb558 of the human NADPH oxidase leading to defective translation of the cytosolic proteins p47-*phox* and p67-*phox*. *J Clin Invest* 1994;93:2120-2126.